SINERGI Vol. 28, No. 2, June 2024: 369-380
http://publikasi.mercubuana.ac.id/index.php/sinergi
http://doi.org/10.22441/sinergi.2024.2.016

Analysis of empirical method for predicting maneuverability of ultra-large container ship using Maneuvering Modelling Group (MMG) model

Rangga Zeinurrohman[1], Andi Trimulyono[1]*, Ardhana Wicaksono[2], Eko Sasmito Hadi[1], Samuel Samuel, Muhammad Luqman Hakim[1], Dedi Budi Purwanto[3]
[1]Department of Naval Architecture, Faculty of Engineering, Universitas Diponegoro, Indonesia
[2]Mitsui O.S.K. Lines, Ltd, Tokyo, Japan
[3]Department of Naval Architecture, Faculty of Marine Technology, Sepuluh Nopember Institute of Technology, Indonesia

Abstract
International Maritime Organization (IMO) provided manoeuvrability standards for all ships above 100 m to ensure the ship's safety and surroundings. In the preliminary design stage, one way to ensure a ship's manoeuvrability under IMO standards is to use empirical methods that are cheaper and less time-consuming than model tests. Empirical methods used analysis regression to develop their formula from the model test result database, and their formula depends on ship hull parameters and dimension ratios such as L/B, C_B, d/B, and $(1-C_B)L/B$. However, the database of the existing empirical formulas is limited to small-medium merchant ships and fishing vessels, as consequences for larger ships are inaccurate and have a significant error in predicting ship manoeuvres. This study modified the existing empirical formulas by adding specified ship data into the existing database and analyzing the accuracy of predicting ship manoeuvres using the Maneuvering Modelling Group (MMG) model. We verify by adding the selected ship data into the existing database, which shows improvement in predicting ship manoeuvres. The modified formulas show improvement by only giving 5% RMSE of tactical diameter and 3% RMSE of ship advance in turning manoeuvre, and this is a 78% overall improvement in predicting the turning motion of ultra-large container ships compared to previous formulas. The quantitative and qualitative produce better estimation result that indicates the right track to derive the empirical formulas for Ultra-Large Container ships.

Keywords:
Empirical;
Maneuverability;
MMG Model;
Ultra-large Container ship;

Article History:
Received: September 25, 2023
Revised: December 21, 2023
Accepted: January 5, 2024
Published: June 2, 2024

Corresponding Author:
Andi Trimulyono
Department of Naval Architecture, Universitas Diponegoro, Indonesia
Email: anditrimulyono@lecturer.undip.ac.id

INTRODUCTION

Manoeuvrability is the most critical aspect for ships because it affects ship safety at sea and influences ship performance. International Maritime Organization (IMO) has a regulation that ships 100 meters long or above must comply with their rule. The regulation applies to all chemical tankers and gas carriers with any rudder and propeller specification. To ensure that the ship's manoeuvrability complies with IMO standards, this must be done during the preliminary design stage, which can be done using various methods.

The International Towing Tank Conference (ITTC) [1] and SIMMAN [2] have collected and recommended several methods for predicting ship manoeuvres that suit the actual conditions. Free Running Model Test (FRMT) is the best method to predict ship manoeuvres, such as zig-zags and turning circles. Maritime Research Institute Netherlands (MARIN) is one organization that provides general ship data such as KVLCC1 & 2, KCS, and DTMB 5415 using the FRMT method. Apart from using the FRMT method, the CFD method to predict ship manoeuvres is starting to develop over time [3, 4, 5, 6]. This approach can simulate the condition of a ship when manoeuvring according to its original requirements but requires quite a large number of resources to complete the simulation. Apart from these methods, other prediction methods are widely used by academics and industry, such as identification systems [7, 8, 9, 10, 11] and mathematical models [12, 13, 14, 15] to model ship manoeuvre movements.

The Maneuvering Modelling Group (MMG) model is a manoeuvre simulation approach that models ship manoeuvres into mathematical functions. MMG model used a basic mathematical equation to model ship manoeuvres into three degrees of freedom (DOF): sway, surge, and yaw. MMG model has been used in the marine industry to predict the manoeuvre of small passenger ferries [16], and the method accurately predicts ship manoeuvres in the preliminary design stage if compared with FRMT or open water test.

Some hydrodynamics coefficients are needed when simulating the ship's manoeuvre using the MMG model. The hydrodynamics coefficients can be obtained by captive model tests, CFD, towing tank tests, or using the Empirical Prediction Method (EMP). EMP uses the database of the ship's form and ratio of dimension parameters to derive the empirical formula, so the formula's accuracy in obtaining or predicting the ship's hydrodynamics coefficients depends on the database used.

There are some empirical formulas to predict the hydrodynamics coefficients that can be used for general and specified type ships [7, 8, 17], yet the formulas are limited due to the range of databases used to derive the formula. The empirical databases are limited to various ship types, including fishing vessels and some medium merchant ships. There are fewer databases of large ships, especially 200 meters or above, for predicting its hydrodynamics coefficient. This study aimed to ensure the prediction of the hydrodynamics coefficient of larger vessels can be accurately estimated.

METHODS

Equations of Motion & Coordinate System

This study used the 3 DOF MMG model, i.e. surge, sway, and yaw motion into three equations of motion [17] which can be seen in (1). MMG Model equations are calculated in time domain simulation, which means every force, moment, or translation that occurs in the present time step will affect the result calculation of the next time step. Figure 1 shows the coordinate system used in the MMG model from the right-handed Cartesian coordinate system, $o_0 - x_0 y_0 z_0$ is for earth fixed coordinate with x_0 & y_0 are calm water, and $o - xyz$ is ship coordinate with o placed at midship. Here z_0 is oriented vertically downwards in the $x_0 - y_0$ plane, and z is oriented vertically downwards in the $x - y$ plane.

The heading angle (ψ) is defined as the angle between x_0 and x axis, δ is the rudder angle to the x axis, and r is the ship's yaw rate. u and v are longitudinal and lateral velocity components and U is the resultant velocity at the midship $\left(U = \sqrt{u^2 + v^2}\right)$. β is the drift angle that is defined as $\beta = tan^{-1}(-v/u)$.

$$\begin{aligned} (m+m_x)\dot{u} - (m+m_y)vr &= X_H + X_R + X_P \\ (m+m_y)\dot{v} + (m+m_x)ur &= Y_H + Y_R \\ (I_{zz}+J_{zz})\dot{r} &= (N_H + N_R) - x_G(Y_H + Y_R) \end{aligned} \quad (1)$$

Subscript *H*, *R*, and *P* refer to the force component acting on the hull, rudder, and propeller. m is mass of ship, I_{zz} is moment of inertia of ship in yaw motion; m_x, m_y, and J_{zz} are added mass and added moment inertia respectively. x_G represents the location of center gravity of ship in x-direction.

In this study, hydrodynamic forces and moment, mass, added mass, moment of inertia, added moment of inertia, and other kinematical parameters are calculated using a non-dimensional form that is indicated by ' (prime) sign.

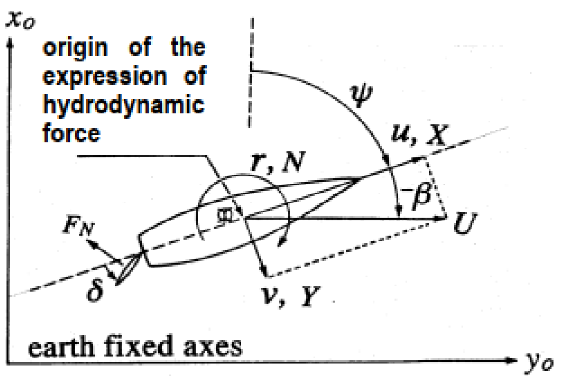

Figure 1. Coordinate system [7]

Table 1. The non-dimensionalization of ship and kinematical parameters

Parameters	Non-dimensionalized by
X, Y	$1/2\,\rho L d U^2$
N	$1/2\,\rho L^2 d U^2$
u, v	U
r	U/L
m, m_x, m_y	$1/2\,\rho L d$
I_{zz}, J_{zz}	$1/2\,\rho L^2 d$
x_G	L

Table 1 shows the non-dimensionalization of a ship and kinematical parameters with L as the ship length perpendicular, d as the ship draft, and ρ as the sea water density (1.025 kg/m^3).

Hull force components

The nondimensional hull force is divided into longitudinal (X'_H), transversal (Y'_H), and ship moment (N'_H) components. The forces are expressed in polynomial functions of v' and r'.

$$\begin{aligned} X'_H &= -R'_0 + X'_{vv}r'^2 + (X'_{vr} - m'_y)v'r' \\ &\quad + (X'_{rr} + x'_G m'_x)r'^2 \\ &\quad + X'_{vvv}v'^4 \\ Y'_H &= Y'_v v' + (Y'_r - m'_x)r' + Y'_{vvv}v'^3 \\ &\quad + Y'_{vvr}v'^2 r' + Y'_{vrr}v'r'^2 \\ &\quad + Y'_{rrr}r'^3 \\ N'_H &= N'_v v' + N'_r r' + N'_{vvv}v'^3 + N'_{vvr}v'^2 r' \\ &\quad + N'_{vrr}v'r'^2 + N'_{rrr}r'^3 \end{aligned} \tag{2}$$

Based on (2), X'_{vv}, X'_{vr}, X'_{rr}, X'_{vvv}, Y'_v, Y'_r, Y'_{vvv}, Y'_{vvr}, Y'_{vrr}, Y'_{rrr}, N'_v, N'_r, N'_{vvv}, N'_{vvr}, N'_{vrr}, and N'_{rrr} are the hydrodynamics coefficients that affect the ship's maneuverability in X-axis, Y-axis, and N-moment. The R'_0 is the resistance coefficient that can be obtained with the empirical formula such as Holtrop or flat plate resistance.

Propeller force components

The surge motion that works on the hull is generated by propeller force in the x-axis can be seen in (3)-(6).

$$X_p = (1 - t_P)T \tag{3}$$

$$T = \rho n_P^2 D_P^4 K_T \tag{4}$$

$$K_T(J_P) = k_2 J_P^2 + k_1 J_P + k_0 \tag{5}$$

$$J_P = \frac{u(1 - w_P)}{n_P D_P} \tag{6}$$

T is the propeller thrust that described in (4) with n_P as propeller rotation per second (RPS), D_P as propeller diameter, and K_T as propeller thrust coefficient. The thrust coefficient in this study is defined in polynomial 2nd order in (5) respectively to speed advance of the propeller (J_P). The values of k_2, k_1, and k_0 are propeller characteristics that can be obtained from the propeller open water test. The w_P and t_P are the wake deduction factor and thrust deduction factor respectively that value can be obtained from a captive test model or empirical approach.

Rudder force components

The forces that are generated by the movement of the rudder are divided into longitudinal and lateral force components (X_R & Y_R) and ship moment (N_R) that can be expressed in (7). t_R is the steering resistance deduction factor. a_H and x_H are rudder force increase factor and the longitudinal location of a_H. Based on the towing tank test, the value of a_H is varied around 0.3-0.4 depending on the hull and rudder geometry [18]. x_H can well estimated $-0.45L$ (the negative value means the position is behind the midship) [19]. x_R represents the location of the rudder behind the midship ($x_R = -0.5L$).

$$\begin{aligned} X_R &= -(1 - t_R)F_N \sin\delta \\ Y_R &= -(1 + a_H)F_N \cos\delta \\ N_R &= -(x_R + a_H x_H)F_N \cos\delta \end{aligned} \tag{7}$$

$$F_N = \left(\frac{1}{2}\right)\rho A_R U_R^2 f_a \sin(\alpha_R) \tag{8}$$

F_N in (8) is the rudder normal force expressed based on lift theory influenced by rudder inflow angle (α_R); A_R represents the rudder area; U_R is the resultant of longitudinal and lateral inflow velocity at the rudder ($\sqrt{u_R^2 + v_R^2}$) that can be expressed in (9)-(10). ε is the wake fraction ratio; κ is the experimental constant that can be defined as $\kappa = k_x/\varepsilon$ with k_x as the propeller inflow ratio on the rudder; η is the ratio of propeller diameter to rudder height.

$$u_R = \varepsilon u(1 - w_P)\sqrt{\eta\left\{1 + \kappa\left(\sqrt{1 + \frac{8K_T}{\pi J_P^2}} - 1\right)\right\}^2 + (1 - \eta)} \tag{9}$$

$$v_R = U\,\gamma_R\,\beta_R \tag{10}$$

γ_R is the flow straightening coefficient, which is usually smaller than 1.0. This indicates that the flow velocity through the rudder will become smaller as the angle β_R increases as shown in (11). The γ_R value has quite an influence on the predicted results of ship manoeuvres, as results of this value must be obtained accurately from model tests or empirical estimation.

$$\beta_R = \beta - \ell'_R r' \tag{11}$$

$$\alpha_R = \delta - \tan^{-1}\left(\frac{v_R}{u_R}\right) \cong \delta - \left(\frac{v_R}{u_R}\right) \tag{12}$$

$$f_a = 6.13\Lambda/(2.25 + \Lambda) \tag{13}$$

ℓ'_R is a non-dimensional longitudinal coordinate of the rudder position whose value is -0.5 or close to -1.0 [20].

f_a in lift theory equation is written as lift coefficient (C_L). Equation (13) was derived by Fujii [21] by correcting the thin aerofoil formulas with respect to the rudder aspect ratio (Λ).

Choosing the empirical formulas

Empirical formulas are based on model test databases that limit the ship's type or dimensions. Using empirical formulas outside the databases can lead to some degree of error in predicting ship maneuvers. Choosing the correct empirical formulas can be done by analyzing the ship type and dimensions that match the databases of empirical formulas.

Several empirical formulas can be used to estimate the hydrodynamics coefficients, yet not all derived formulas can calculate all the hydrodynamics coefficients for MMG models. The formulas derived by Kijima and Yoshimura [7] [17] are the popular formulas used to estimate the hydrodynamics coefficients because of their wide range of databases. The main dimensions of Kriso Container Ship (KCS) are chosen to represent the dimensions of the large container ship [2].

The formula ranges of ship form and dimensions are shown in Table 2. The Yoshimura empirical formulas are chosen because KCS dimensional ratios satisfy the formula ranges, even the L/B ratio and Cb are in the upper limit of ranges.

Equation (14)-(17) are the Yoshimura empirical formulas [17] to estimate the hydrodynamics coefficients. τ' is the non-dimensional trim that can be expressed as $(\tau' = trim/d_m)$ with $trim$ is how much ship trim by the stern in meters and d_m is ships mean draft. In this study, Equation (14) is the linear hydrodynamics coefficient for trim ship conditions.

$$\left.\begin{aligned} Y'_v &= Y'_{v_0}(1+0.54\tau'^2) \\ Y'_r - m'_x &= (Y'_r - m'_x)_0(1+1.82\tau'^2) \\ N'_v &= N'_{v_0}(1-0.85\tau') \\ N'_r &= N'_{r_0}(1-0.33\tau') \end{aligned}\right\} \quad (14)$$

$$\left.\begin{aligned} Y'_{v_0} &= 0.5\pi k + 1.4(C_B B/L) \\ (Y'_r - m'_x)_0 &= 0.5(C_B B/L) \\ N'_{v_0} &= k \\ N'_{r_0} &= -0.54k + k^2 \end{aligned}\right\} \quad (15)$$

Table 2. The ideal range of ratio for ship form

	KCS	Kijima	Yoshimura & Masumoto
L/B	7.14	4.5 – 6.81	2.6 – 7.1
d/B	0.34	0.24 – 0.42	0.25 – 0.46
Cb	0.65	0.52 – 0.84	0.51 – 0.65

$$\left.\begin{aligned} X'_{vv} &= 1.15(C_B B/L) - 0.18 \\ X'_{vr} - m'_y &= 1.91(C_B B/L) + 0.08 \\ X'_{rr} + x'_G m'_y &= -0.085(C_B B/L) + 0.008 \\ X'_{vvvv} &= -6.68(C_B B/L) + 1.10 \end{aligned}\right\} \quad (16)$$

$$\left.\begin{aligned} Y'_{vvv} &= 0.185L/B + 0.48 \\ Y'_{vvr} &= 0.97\tau'/C_B - 0.75 \\ Y'_{vrr} &= 0.26(1-C_B)L/B + 0.11 \\ Y'_{vrr} &= 0.069\tau' - 0.051 \\ N'_{vvv} &= -0.69C_B + 0.66 \\ N'_{vvr} &= 1.55(C_B B/L) - 0.76 \\ N'_{vrr} &= 0.075(1-C_B)L/B - 0.098 \\ N'_{rrr} &= 0.25(C_B B/L) - 0.056 \end{aligned}\right\} \quad (17)$$

With: $k = 2d/L$

Modified Empirical Formulas

The empirical formulas are sensitive to databases used to derive the formulas. The Yoshimura databases include fishing vessels, training ships, and medium merchant vessels. The wide range of ship types and limited ship dimensions have some degree of error because from Table 2 shows that KCS ratios and form parameters are in the upper limit.

Container ships are typically long and slender and also have Cb around 0.6-0.7. This characteristic can affect the hydrodynamics coefficients as shown in (14)-(17). As shown in Figure 2, the KCS L/B ratio is at the upper limit and far away from the Yoshimura database trend line.

Selection of new ship dimensions

When modifying the Yoshimura formulas, the first thing to do is make the KCS dimensions ratio more ideal. Thirteen new ships that can be seen in Table 3 are substituted into the existing databases of Yoshimura. Three types of container ships are meant to expand the range of derived formulas.

Figure 2 shows the database has become more ideal for KCS. The range of Cb is increasing up to 0.74 and L/B to 7.6. This also shows the container type has different characteristics from fishing vessels, training ships, or tankers [17]. Figure 3 shows that container vessels tend to have a low d/B ratio, this is because the container ship requires a high transverse stability caused by high loads above the deck compared to fishing boats and tankers that are loaded below the deck. Figure 4 shows that the *k* coefficient of new ship data was lower compared to Yoshimura ship data although for d/B ratio is comparable. This is because the new data ship was based on the latest large merchant ship.

Table 3. New ship Parameters

L	d	Cb	L/B	Type
206.20	11.20	0.63	6.287	
214.00	11.53	0.56	6.646	
217.30	12.45	0.63	5.826	
240.00	12.03	0.61	7.059	
245.15	19.30	0.62	7.602	*Feedermax*
258.00	14.50	0.65	6.028	
264.40	14.00	0.59	6.610	
286.70	12.52	0.60	7.168	
287.00	15.00	0.69	5.948	
309.20	14.50	0.64	7.224	
319.00	15.00	0.65	7.453	*Panamax*
350.00	16.00	0.74	7.261	
381.40	16.00	0.74	7.063	*New-Panamax*

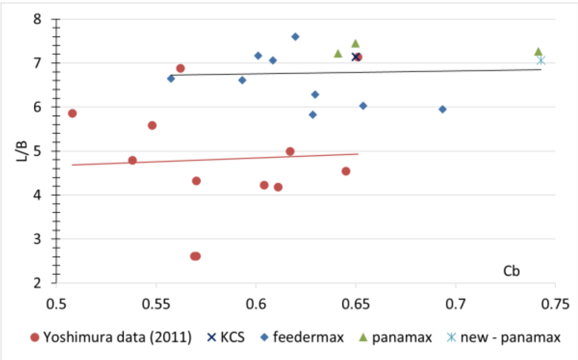

Figure 2. Ships database comparison

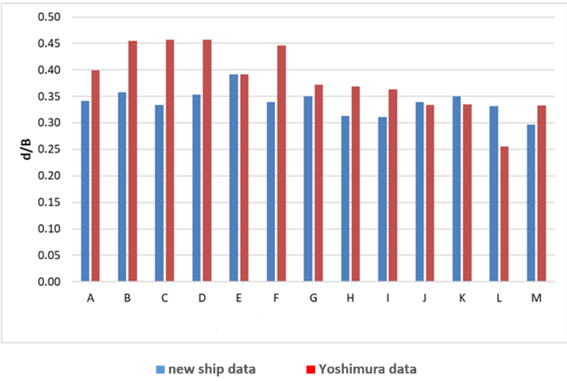

Figure 3. Comparison of d/B ratio

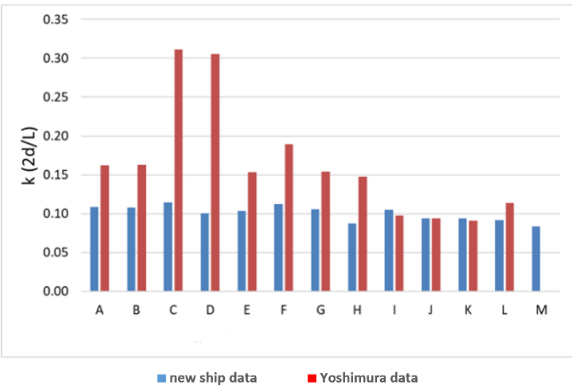

Figure 4. Comparison of k ratio

Modification of empirical formula

The ideal method to derive the empirical formula using the analytical method is by following the steps of similar studies [7, 8, 17]. However, due to the lack of model test results of the large container ship, this study gathered the hydrodynamic coefficients of thirteen new ships data using the chosen empirical method in (15)-(17).

In the process, all ship's main parameters that have high correlations with the hydrodynamic coefficient are identified. The value of L/B represents the purpose of construction and can be varied. $C_b/(L/B)$ is the ratio of the coefficient Cb which represents the level of hull contrast to L/B and represents the unique characteristics of the hull [3].

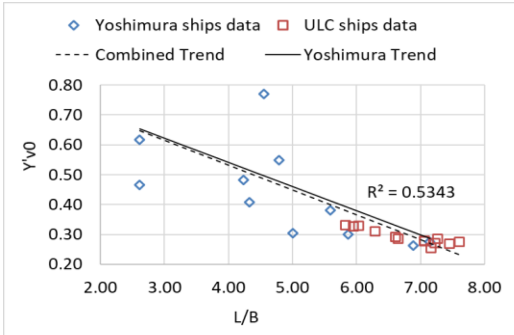

Figure 5. Correlation $\mathrm{Y'}_{\mathrm{v}_0}$ to ship's parameter

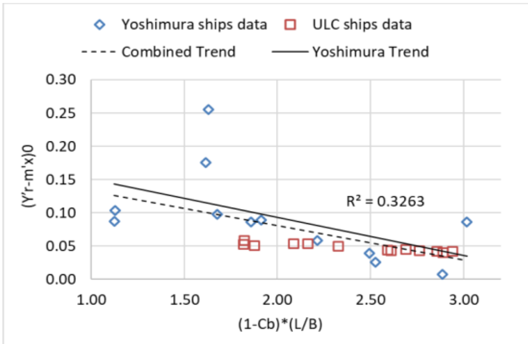

Figure 6. Correlation $(\mathrm{Y'_r} - \mathrm{m'_x})_0$ to ship's parameter

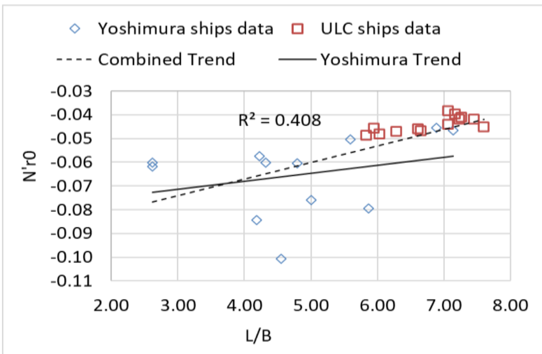

Figure 7. Correlation $\mathrm{N'_{v_0}}$ to ship's parameter

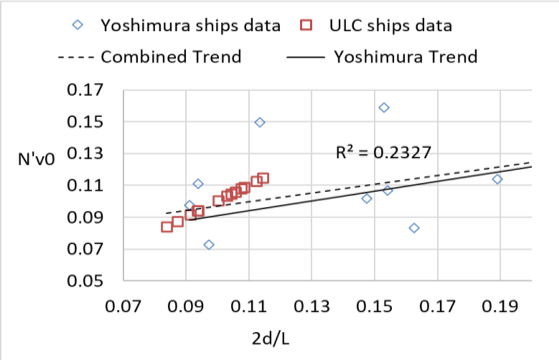

Figure 8. Correlation N'_{r0} to ship's parameter

Figure 5, Figure 6, Figure 7 and Figure 8 show the relationship between the twenty-six ship's data (thirteen ships from Yoshimura data and thirteen ships from new container data) linear hydrodynamic coefficients (15) and the ship's parameters. By using trend line correction to derive the empirical formula, it can be concluded that the lateral force value is strongly influenced by the parameter $(1-C_b)(L/B)$ and the yaw moment value tends to be at a low $2d/L$. From Figure 5, Figure 6, Figure 7 and Figure 8, it can also be concluded that the previous approach [17] for merchant ships, especially container ships, with large sizes has the potential to experience errors in predicting their maneuverability due to differences in ship parameters and characteristics from fishing ships, Ro-Ro, or car-carrier.

In the same way, the non-linear hydrodynamic coefficients are modified to optimize the empirical formulas. The derived formula can be shown in (18)-(20). Even though it has been optimized, the formulas have the ideal limit of the ship's parameters to estimate the hydrodynamic coefficients. Using modified formulas outside the limits can result in a high error rate in predicting the hydrodynamic coefficients and lead to low accuracy of the ship maneuver prediction. Should be noted that (14) is not being modified considering ships in fully loaded condition most likely don't have large trim.

$$5.35 < L/B < 7.6\ ;$$
$$0.56 < C_b < 0.74\ ;$$
$$0.084 < k < 0.115\ ;$$
$$1.817 < (1-C_b)(L/B) < 2.941$$

$$\left.\begin{aligned} Y'_{v0} &= -0.083(L/B) + 0.8638 \\ (Y'_r - m'_x)_0 &= -0.052(1-C_B)(L/B) + 0.1849 \\ N'_{v0} &= 0.274k + 0.0696 \\ N'_{r0} &= 0.0069(L/B) - 0.0948 \end{aligned}\right\} \quad (18)$$

$$\left.\begin{aligned} X'_{vv} &= 1.1337[C_B/(L/B)] - 0.1804 \\ X'_{vr} - m'_y &= -1.8786[C_B/(L/B)] + 0.075 \\ X'_{rr} + x'_G m'_y &= 0.0081(1-C_B)(L/B) - 0.00203 \\ X'_{vvvv} &= -6.878[C_B/(L/B)] + 1.0851 \end{aligned}\right\} \quad (19)$$

$$\left.\begin{aligned} Y'_{vvv} &= 0.1825(L/B) + 0.5001 \\ Y'_{vvr} &= -0.6252(1-C_B)(L/B) + 0.8965 \\ Y'_{vrr} &= 0.2498(1-C_B)(L/B) + 0.1392 \\ Y'_{rrr} &= -0.083(L/B) + 0.8638 \\ N'_{vvv} &= -0.722573C_B + 0.684259 \\ N'_{vvr} &= 1.4338[C_B/(L/B)] - 0.757 \\ N'_{vrr} &= 0.0729(1-C_B)(L/B) - 0.0913 \\ N'_{rrr} &= 0.2376[C_B/(L/B)] - 0.0554 \end{aligned}\right\} \quad (20)$$

Validation of The Modified Empirical Formulas

Validating the modified formulas can be done by simulating the ship maneuvers using the MMG model. Besides the hydrodynamic coefficients, the MMG model needs hull-propeller-rudder interaction coefficients to calculate (3), (5), (6), and (7). Table 4 shows the estimation methods that are suitable for large ships.

The validation using Kriso Container Ship (KCS), the parameters and dimensions [2] can be seen in Table 5. The validation criteria that are carried out include maneuver trajectory, turning parameter, and ship's overshoot angle. Note that the validation was performed in ideal conditions suggested by IMO [22].

The process of simulating the ship's maneuver can be seen in Figure 9. Note that the simulation results depend on how accurate the estimation coefficients and time-step configuration are. Failure of the simulation result may occur because of poor time-step configuration or inaccurate coefficient estimation.

Table 3. Estimation method used for estimating interaction coefficient

Reference	Coefficients
JASNAOE. [12]	Open water characteristics (k_0, k_1, & k_2)
Harvald. [23]	Wake Fraction Ratio (w_P)
Molland et al. [24]	Thrust Deduction Factor (t_P)
Lee et al. [25]	• Flow Straightening Coefficient (γ_R) • Wake Fraction Ratio (ε) • Steering resistance deduction factor (t_R) • Rudder force increase factor (a_H) • Experimental constant (κ) • Non-dimensional longitudinal coordinate of the acting point of the additional lateral force (x'_H)

Table 4. KCS parameters and dimensions

Parameters	Dimensions
Model scale	1:1
Length perpendicular (L)	230 m
Breadth (B)	32.2 m
Draft (d)	10.8 m
Displacement (∇)	52,030 m^3
Coefficient block (Cb)	0.651
LCG	111.6 m
Test speed	24 knots
Propeller Diameter (Dp)	7.9 m
P/Dp	0.997
Ruder Lateral Area (A_R)	54.45 m^2
Rudder Height (H_R)	9.90 m
Rudder Aspect Ratio (Λ)	1.80
Rudder Turn Rate	2.32 deg/s

This study refers to ITTC [26] as the standard for choosing several time steps to obtain a suitable time-step configuration. This study uses (21) for standard pseudo-transient resistance computations as the basic formula to choose the optimal time steps.

$$\Delta t = 0.005 \sim 0.01\frac{L}{U} \tag{21}$$

Table 6 shows the several time steps that were chosen. The result of ship advance and tactical diameter are shown in non-dimensional form. The result showed the calculation becomes steady from one hundred time steps to ten thousand time steps. Considering the calculation time simulation, this study uses a one-hundred-time-step configuration.

Table 7 and Figure 10 shows the comparison results of the turning motion simulation from modified formulas, Kijima [7], Yoshimura [17], and the experiment captive model test [12]. The modified formulas have similar turning test results compared to the Yoshimura formulas with slight improvement for ship advance, the turning trajectory satisfied the IMO regulations and matched the experiment data performed by the captive model test. Figure 11 shows the overshoot angle (OSA) of the modified formulas result is 3.24° for 1st OSA and 3.26° for 2nd OSA, smaller than the experiment result of 5.79° for 1st OSA and 10.44° for 2nd OSA.

Table 5. The result of KCS turning maneuvers with several different time step variations

	KCS Turning Result	
Time steps	Ship Advance	Tactical Diameter
0.0250	3.8131L	4.2494L
0.0100	3.2565L	4.0360L
0.0050	3.2775L	4.0446L
0.0001	3.2560L	4.0361L

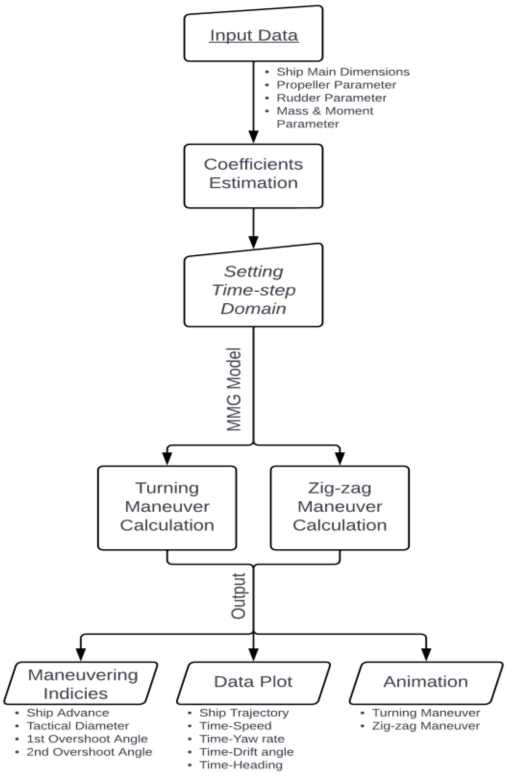

Figure 9. Structure of maneuver simulation process

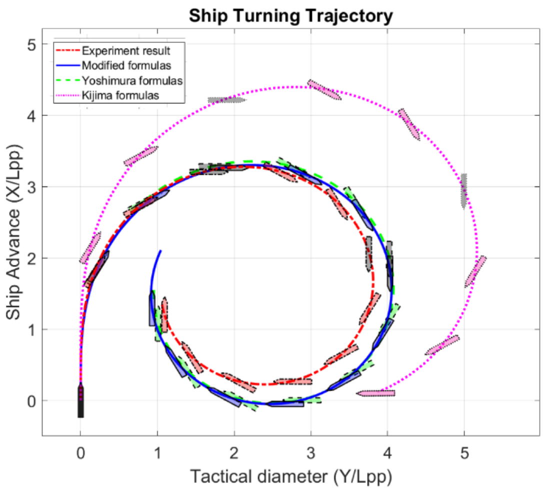

Figure 10. Comparison of KCS Turning Test trajectories

Table 6. Quantitative Comparison of turning test results on KCS ships

		Tactical Diameter	***Ship Advance***
Experiment		3.75L	3.22L
Modified formulas	Result	4.03L	3.28L
	RMSE	**20%**	**4%**
Yoshimura formulas	Result	4.02L	3.30L
	RMSE	**19%**	**6%**
Kijima formulas	Result	4.98L	4.22L
	RMSE	**87%**	**71%**
IMO criteria		5.00L	4.50L

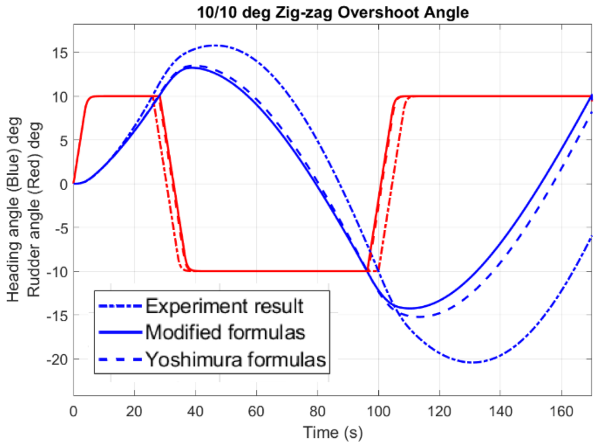

Figure 11. Comparison of Overshoot angle KCS 10°/10° Zig-zag Test

RESULTS AND DISCUSSION

This research aims to minimize estimation errors that may occur at the preliminary design stage on larger ships when using empirical formulas intended for smaller vessels. Figure 10 shows a slight improvement in maneuver from the modified empirical formulas, this may be caused by the validation subject that is considered the medium container ship. In addition to checking the improvement of the modified formulas compared to previous formulas, the 2015 ULC ship Maersk Sirac, with a capacity of 10,000 TEU, is the subject of testing for modified empirical methods that the dimension showed in Table 8.

Derived The Hydrodynamic and Interaction Coefficients

The hydrodynamic and interaction coefficients were derived from modified formulas and Yoshimura formulas as a comparison [17]. Table 9 shows the hydrodynamic coefficients of ULC derived from modified formulas, Yoshimura formulas, and Pipchenko, which derived the coefficients based on the sea trial test [27]. Some of the interaction coefficients from the sea trial test are not available from Pipchenko in Table 9.

Table 7. Ship parameters of Maersk Sirac [27]

Parameters	Dimensions
Length perpendicular (L)	287 m
Breadth (B)	48.2 m
Mean Draft (d)	12.5 m
Trial Aft Draft	10.16 m
Trial Fwd Draft	4.02 m
Wet Surface Area	11656 m^2
Coefficient block (Cb)	0.604
Propeller Diameter (Dp)	9.7 m
Rudder Area (A_R)	78.95 m^2

Table 8. Hydrodynamic and interaction coefficients

	Sea Trial by Pipchenko	Modified formula	Yoshimura formula
Hydrodynamic coefficients			
X'_{vv}	-0.2617	-0.0654	-0.0634
X'_{vr}	-0.1531	-0.1156	-0.1137
X'_{rr}	-0.0007	-0.0021	-0.0006
X'_{vvv}	0.4781	0.3874	0.4224
Y'_{v}	0.1044	0.4901	0.3030
Y'_{r}	0.1795	0.1307	0.1065
Y'_{vvv}	2.7160	1.5867	1.5815
Y'_{vvr}	0.9423	-0.5776	0.4982
Y'_{vrr}	1.3620	0.7282	0.7231
Y'_{rrr}	0.0010	0.3695	-0.0510
N'_{v}	0.0087	0.0287	0.0187
N'_{r}	-0.0300	-0.0675	-0.0335
N'_{vvv}	0.2259	0.2478	0.2432
N'_{vvr}	-0.6445	-0.6116	-0.6028
N'_{vrr}	0.1090	0.0806	0.0788
N'_{rrr}	-0.0550	-0.0313	-0.0306
Interaction coefficients			
ε	1.3440	1.2923	0.9169
a_H	0.3422	0.2918	0.3652
γ_R	0.3120	0.2973	0.3490
t_R	N/A	-0.2809	-0.8587
x'_H	N/A	-0.4533	-0.4000
κ	N/A	0.3593	0.5997
k_x	N/A	0.4643	0.5500
ℓ'_R	N/A	-1.0000	-0.9000

The empirical formulas may have differences in predicting hydrodynamic and interaction coefficients. This is due to the limitations of the database used to derive the formulas. An accurate estimation can be obtained for hull forms that are similar or equivalent to the ones used in the database of the empirical formula. In contrast, the accuracy tends to suffer when applying the formula to a different hull form. To verify the improvement of empirical formulas, all the coefficients were derived from modified formulas and Yoshimura formulas without any additional correction.

Maneuverability Evaluation and Maneuver Conditions

To evaluate the ship's maneuvers, the testing conditions must meet the criteria below [22]:

1. Calm waters without restrictions;
2. Deepwater;
3. Fully loaded condition;
4. Performed at a constant speed.

In reality, fulfilling the above conditions was impossible, especially for sea trial testing. These differences in conditions can affect the maneuver results from what was expected. However, this study aims to verify the modified formulas, so we decided to ignore the external factors that occur in the present study. For information, Table 10 shows the comparison of sea trial and simulation conditions

Table 9. Maneuverability evaluation conditions.

	Sea Trial	Simulation
Wind & current	N/A	Calm
Water depth	Deepwater	Deepwater
Ship's draft	After: 10.16 m Fore: 4.02 m	After: 10.16 m Fore: 4.02 m
Ship's speed	≈22 kn	22 kn

. It can be seen the same condition of maneuverability was carried out to directly compare our models with the experiment conditions. As a result, the modified formulas indicated the real condition of the ship manoeuvre.

Turning Motion Test

Table 11 and Figure 12 show the modified formulas have smaller tactical diameters and ship advance values than Yoshimura formulas. Both the modified formulas and Yoshimura formulas turning simulation satisfy the IMO regulation, yet the modified formulas show a smaller RMSE of tactical diameter that indicates the improvement of prediction. However, the absolute turning diameter of modified formulas was still more prominent than the sea trial result, this correlated to the ship's speed deceleration. Similar results were shown for Yoshimura formulas, the turning test trajectories showed overestimates compared to sea trial results. It can be explained that our database parameters are slightly difference as shown in Figures 3 and 4 creating a large difference between Yoshimura's results

Figure 13 shows the speed deceleration of the sea trial results down to 64%, this happened because of drag generated from the rudder plate and around the hull during the turning motion [8]. However, the modified formulas experienced only 36% speed deceleration, or 28% smaller speed deceleration than the sea trial result. This may occur because the modified formulas were derived based on the formulas that are suitable for general ship type, it is common sense that reduction in the initial speed can be around 30–40% for general ships and as much as 70–80% for VLCC and ULCC [28][29].

The amount of yaw rate in Figure 14 correlated to the speed deceleration. As can be seen in the 400 second, there is a 'spike' that occurs, if considering the condition in Table 10, this may happen because of some sort of wave, current, or wind that affects the ship's performance.

Table 10. Quantitative Comparison of turning test results on ULC ship

		Tactical Diameter	Ship Advance
Sea Trial		4.05L	2.87L
Modified formulas	Result	4.12L	2.83L
	RMSE	**5%**	**3%**
Yoshimura formulas	Result	4.94L	3.19L
	RMSE	**63%**	**23%**
IMO criteria		5.00L	4.50L

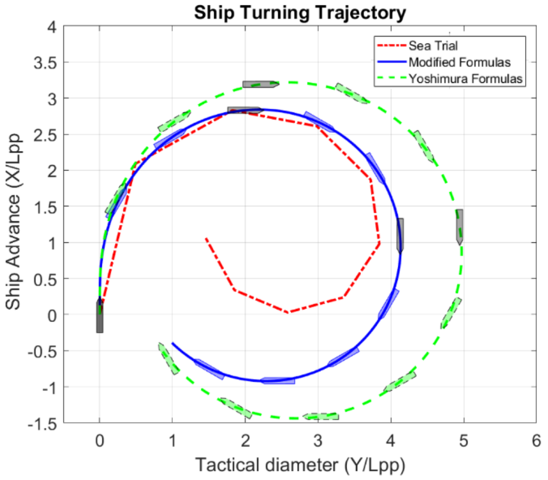

Figure 12. Comparison of the turning test trajectories ULC ship

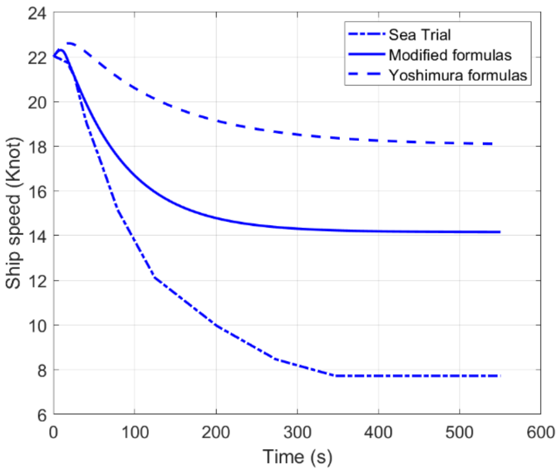

Figure 13. Comparison of the speed deceleration during the turning test ULC ship

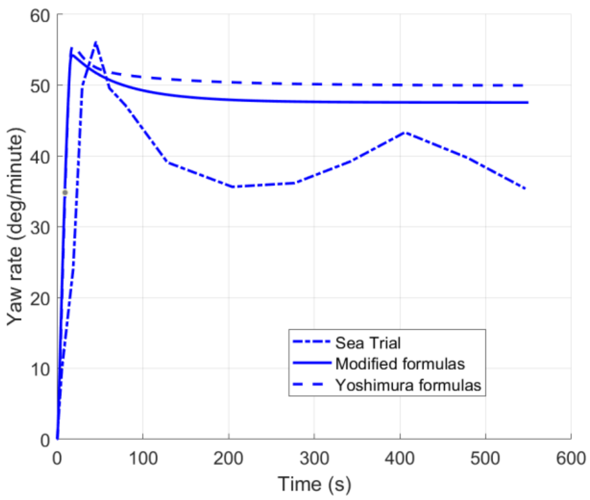

Figure 14. Comparison of the yaw rate during the turning test ULC ship

10°/10° Zigzag Test

Table 12 and Figure 15 show that both the modified and Yoshimura formulas satisfy the IMO criteria on the 10°/10° zig-zag test. However, both overshoot angle results are smaller than observed. Notice that the initial turning of modified formulas is 5 s faster than observed, this may correlate to Figure 14, that the modified formulas have faster yaw rates than the observed result. It showed that the present study has acceptable results compared to the study by Yoshimura for the zig-zag test.

Although some significant differences exist in yaw rate and speed deceleration. In addition, turning maneuvers show acceptable compared to Yoshimura results for both KCS and ULC ships it can be concluded our modified empirical formulas were acceptable for the present study.

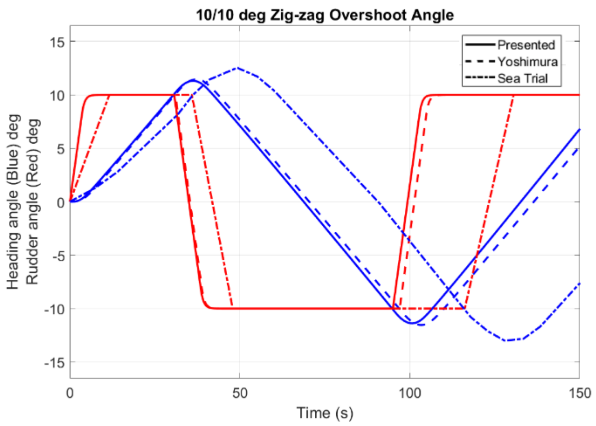

Figure 15. Comparison of overshoot angle 10°/10° zigzag test ULC ship

Table 11. Quantitative comparison of 10°/10° zigzag test results on ULC ship

		1st OS	2nd OS
Sea Trial		2.50°	3.20°
Modified formulas	Result	1.07°	1.16°
	Difference	**1.43°**	**1.34°**
Yoshimura formulas	Result	1.22°	1.28°
	Difference	**1.28°**	**1.22°**
IMO Criteria		11.51°	27.29°

CONCLUSION

Due to the lack of empirical formulas derived for ultra-large container ships, the present study modifies the empirical formulas originally derived for general ships by adding 13 ultra-large container ships data into the existing database. The hydrodynamic and interaction coefficients of the new database were corrected, and the modified formulas were derived using regression.

The modified formulas show improvement by only giving 5% RMSE of tactical diameter and 3% RMSE of ship advance in turning manoeuvre, this is a 78% overall improvement in predicting the turning motion of ultra-large container ships compared to Yoshimura formulas. Although the steady turning diameter and zig-zag overshoot angles are still quite off the observed result, this finding suggests that the latter quantitatively and qualitatively produces better estimation.

We verify by adding the specified ship data into the existing database, which shows improvement in predicting ship manoeuvres. Although there is still some inaccuracy in estimating the coefficients that lead to inaccuracy of maneuvers results, the result indicates the right track to derive the empirical formulas for Ultra-Large Container ships. More in-depth studies can be conducted to improve the modified formula by using model tests, numerical simulations, or considering the non-linear ship parameters that could affect the ship maneuvers.

REFERENCES

[1] ITTC, “Final Report and Recommendations to the 28th ITTC,” 2017.

[2] SIMMAN, “Workshop on verification and validation of ship manoeuvring simulation methods,” South Korea, 2020.

[3] A. Trimulyono, M. L. Hakim, C. Ardhan, S. T. P. Ahmad, T. Tuswan, and A. W. B. Santosa, “Analysis of the double steps position effect on planing hull performances,” *Brodogradnja*, vol. 74, no. 4, pp. 41–72, 2023, doi: 10.21278/brod74403.

[4] Samuel, A. Trimulyono, P. Manik, and D. Chrismianto, “A numerical study of spray strips analysis on fridsma hull form,” *Fluids*,

vol. 6, no. 11, Nov. 2021, doi: 10.3390/fluids6110420.

[5] A. Wicaksono and M. Kashiwagi, "Wave-induced steady forces and yaw moment of a ship advancing in oblique waves," *Journal of Marine Science and Technology (Japan)*, vol. 23, no. 4, pp. 767–781, 2018, doi: 10.1007/s00773-017-0510-6.

[6] S. Samuel *et al.*, "Investigation of An Inverted Bow on Frigate Hull Resistance," *Journal of Applied Fluid Mechanics*, vol. 17, no. 1, pp. 136–147, 2024, doi: 10.47176/jafm.17.1.2122.

[7] K. Kijima, T. Katsuno, Y. Nakiri, and Y. Furukawa, "On the manoeuvring performance of a ship with the parameter of loading condition," *Journal of the Society of Naval Architects of Japan*, no. 168, pp. 141–148, 1990 doi : https://doi.org/10.2534/jjasnaoe1968.1990.168_141.

[8] S. H. Kim and C. K. Lee, "Estimation of maneuverability of trawl fishing vessel using an analytical method," *Journal of Marine Sciences and Engineering*, vol. 9, no. 8, Aug. 2021, doi: 10.3390/jmse9080854.

[9] S.-H. Kim, C.-K. Lee, and M.-G. Lee, "A study on the improvement of the accuracy of fishing trawlers maneuverability estimation at the design stage," *Journal of the Korean Society of Fisheries Technology*, vol. 56, no. 4, pp. 374–383, 2020, doi: 10.3796/ksfot.2020.56.4.374.

[10] Y. Higo, M. Sakano, H. Nobe, and H. Hashimoto, "Development of trajectory-tracking maneuvering system for automatic berthing/unberthing based on double deep Q-network and experimental validation with an actual large ferry," *Ocean Engineering*, vol. 287, 2023, doi: 10.1016/j.oceaneng.2023.115750.

[11] H. Shen, H. Hashimoto, A. Matsuda, Y. Taniguchi, D. Terada, and C. Guo, "Automatic collision avoidance of multiple ships based on deep Q-learning," *Applied Ocean Research*, vol. 86, pp. 268–288, May 2019, doi: 10.1016/j.apor.2019.02.020.

[12] D. Wardianto, M. Sufiyanto, R. K. Arief, H. A. Prabowo,I. Hilmy "The model selection of propeller turbine construction using Analytical Hierarchy Process (AHP)," *SINERGI*, vol. 27, no. 3, pp. 361-370, 2023. doi: 10.22441/sinergi.2023.3.007

[13] A. H. Muhammad, D. Paroka, S. Rahman, and M. R. Firmansyah, "Pengaruh Sudut Kemiringan dan Jarak antar Daun Kemudi Terhadap Kinerja Maneuvering KMP Bontoharu," *Kapal: Jurnal Ilmu Pengetahuan dan Teknologi Kelautan*, vol. 16, no. 3, pp. 106–114, 2019, doi: 10.14710/kapal.v16i3.24946.

[14] D. Paroka, A. H. Muhammad, and S. Rahman, "Estimation of Effective Wave Slope Coefficient of Ships with Large Breadth and Draught Ratio," *Kapal: Jurnal Ilmu Pengetahuan dan Teknologi Kelautan*, vol. 17, no. 1, pp. 40–49, 2020, doi: 10.14710/kapal.v17i1.28399.

[15] Y. Xia, S. Zheng, Y. Yang, and Z. Qu, "Ship Maneuvering Performance Prediction Based on MMG Model," in *IOP Conference Series: Materials Science and Engineering*, Institute of Physics Publishing, 2018. doi: 10.1088/1757-899X/452/4/042046.

[16] A. Wicaksono, N. Hashimoto, and T. Takahashi, "Representation of small passenger ferry maneuvering motions by practical modular model," *International Journal of Naval Architecture and Ocean Engineering*, vol. 13, pp. 57–64, 2021, doi: 10.1016/j.ijnaoe.2020.12.006.

[17] Y. Yoshimura and Y. Masumoto, "Hydrodynamic Force Database with Medium High Speed Merchant Ships Including Fishing Vessels and Investigation into a Manoeuvring Prediction Method," *Journal of the Japan Society of Naval Architects and Ocean Engineers*, vol. 14, pp. 63–73, 2011, doi: 10.2534/jjasnaoe.14.63.

[18] K. Kose, A. Yumuro, and Y. Yoshimura, "Concrete of mathematical model for ship manoeuvring," in *Proceedings of the 3rd symposium on ship maneuverability*, Society of Naval Architects of Japan, 1981, pp. 27–80.

[19] K. Karasuno, "Studies on the lateral force on a hull induced by rudder deflection," *The Japan Society of Naval Architects and Ocean Engineers Conference*, pp. 14–19, 1969.

[20] H. Yasukawa and Y. Yoshimura, "Introduction of MMG standard method for ship maneuvering predictions," *Journal of Marine Science and Technology (Japan)*, vol. 20, no. 1, pp. 37–52, 2015, doi: 10.1007/s00773-014-0293-y.

[21] H. Fujii and T. Tuda, "Experimental research on rudder performance," *The Japan Society of Naval Architects and Ocean Engineers Conference*, no. 110, pp. 31–42, 1961.

[22] IMO, "Resolution MSC.137 (76) Standards for Ship Manoeuvrability," London, 2002.

[23] S. A. Harvald, *Resistance and Propulsion of Ships*. John Wiley & Sons, 1983.

[24] A. F. Molland, S. R. Turnock, and D. A. Hudson, *Ship Resistance and Propulsion :*

Practical Estimation of Ship Propulsive Power. Cambridge University Press, 2011.
[25] H.-Y. Lee, S.-S. Shin, and D.-J. Yum, "Improvement of Prediction Technique of the Ship′s Manoeuvrability at Initial Design Stage," Journal of the Society of Naval Architecture Korea, vol. 35, 1998.
[26] "ITTC-Recommended Procedures and Guidelines Practical Guidelines for Ship CFD Applications, 2014."
[27] O. Pipchenko, M. Tsymbal, and V. Shevchenko, "Features of an ultra-large container ship mathematical model adjustment based on the results of sea trials," *TransNav*, vol. 14, no. 1, pp. 163–170, 2020, doi: 10.12716/1001.14.01.20.
[28] A. Zullah, T. Dewi, Rusdianasari," Performance analysis of ship mounting PV panels deployed in Sungsang Estuary and Bangka Strait, Indonesia," *SINERGI*, vol. 28, no. 1, pp. 169-182, 2024, doi: 10.22441/sinergi.2024.1.017
[29] J. D. Yoon, Theory and Practice of Ship Manoeuvring. Busan: Sejong Publishing Co., 2019.